



γ -Fe₂O₃@SiO₂@4-(sulfoamino)butanoic acid as a novel superparamagnetic nanocatalyst promoted green synthesis of 5-(aryl)-5*H*-spiro[diindeno[1,2-*b*:2',1'-*e*]pyridine-11,3'-indoline]-2',10,12-trione derivatives

Hadi Mohammadi¹ · Hamid Reza Shaterian¹

Received: 11 June 2018 / Accepted: 17 August 2018
© Springer Nature B.V. 2018

Abstract

Grafting of 4-(sulfoamino)butanoic acid on superparamagnetic γ -Fe₂O₃@SiO₂ nanoparticles afforded γ -Fe₂O₃@SiO₂@4-(sulfoamino)butanoic acid as a novel heterogeneous nanocatalyst, which was characterized by X-ray diffraction, Fourier transform infrared spectroscopy, vibrating sample magnetometry, field emission scanning electron microscopy, and thermal gravimetric analysis. In this research, we report a convenient and one-pot efficient direct protocol for the *pseudo four*-component preparation of 5-(aryl)-5*H*-spiro[diindeno[1,2-*b*:2',1'-*e*]pyridine-11,3'-indoline]-2',10,12-trione derivatives via cascade condensation reaction of 1,3-indandione and isatins with various aromatic amine in the presence of the catalytic amount of γ -Fe₂O₃@SiO₂@4-(sulfoamino)butanoic acid under green conditions in aqueous media. This procedure offers several advantages such as: very easy reaction conditions, simple work-up, or purification, excellent yields, high purity of the desired product, atom economy, and short reaction times. The superparamagnetic catalyst is magnetically separable and retained chemical stability after recycling for at least five consecutive runs without detectable activity loss.

Electronic supplementary material The online version of this article (<https://doi.org/10.1007/s11164-018-3571-1>) contains supplementary material, which is available to authorized users.

Extended author information available on the last page of the article

Graphical abstract



Keywords $\gamma\text{-Fe}_2\text{O}_3@ \text{SiO}_2@ 4\text{-(sulfoamino)butanoic acid}$ · Superparamagnetic nanocatalyst · 5-(Aryl)-5H-spiro[diindeno[1,2-b:2',1'-e]pyridine-11,3'-indoline]-2',10,12-trione · Multi-component reactions

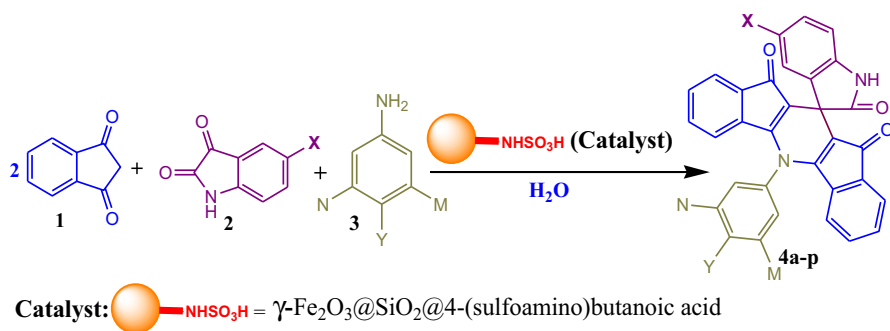
Introduction

Magnetic nanoparticles are of great importance for researchers due to their applications for catalysis [1], biotechnology/biomedicine [2, 3], and magnetic resonance imaging (MRI) [4]. Small naked nanomagnetic particles have a tendency to form agglomerates to reduce the energy associated with the high surface area-to-volume ratio of nanosized particles [5]; this is because they are chemically highly active [6]. Researchers have tried to use protection strategies to chemically stabilize naked magnetic nanoparticles by grafting or coating them with organic species such as polymers [7], or coating with an inorganic layer, such as silica or carbon [8]. The shell-encapsulated nanomagnetic materials can be stabilized and the nanoparticles also used for further organocatalyst functionalizations depending on the desired applications [9]. Functionalized nanomagnetic particles encapsulated by silica have demonstrated potential application as catalysts in organic synthesis [10]. They act as quasi-homogeneous systems for reactions which show high conversion of starting materials to the desired product(s), especially in liquid-phase catalytic reactions [11]. In addition, easy separation of magnetic particles by an external magnet provides a simple reaction work-up produce the desired product(s) in highly pure isolated yields [12]. Thus, functionalization and application of such coated magnetic

nanoparticles in catalysis and easy separation are important to develop these strategies for organic processes and synthesis [13]. Functionalized organocatalysts on nano-superparamagnetic compounds coated by silica are considered a very important class of materials with broad application in many biological aspects [14, 15]. Nano-superparamagnetic transition metal oxides such as iron are one of the most adjustable systems which also have applications in medical, industrial, and biological systems, in addition to their important roles in catalysis and organic synthesis [16–18]. Studies of this new kind of organometallic compound grafting of organocatalysts on superparamagnetic γ -Fe₂O₃@SiO₂ nanoparticles has attracted the consideration of researchers in organic chemistry. In the present research, we report preparation of γ -Fe₂O₃@SiO₂@4-(sulfoamino)butanoic acid for the first time. This superparamagnetic compound as catalyst was applied for synthesizing a series of 5-(aryl)-5*H*-spiro[diindeno[1,2-*b*:2',1'-*e*]pyridine-11,3'-indoline]-2',10,12-trione derivatives via *pseudo* cascade *four*-component condensation reaction of 1,3-indandione and isatins with various aromatic amines in the presence of a catalytic amount of γ -Fe₂O₃@SiO₂@4-(sulfoamino)butanoic acid under green conditions in aqueous media (Scheme 1).

Experimental

All materials were purchased from Merck and Aldrich Companies. Nuclear magnetic resonance (NMR) spectra were determined using a Bruker Avance 300 MHz instruments in DMSO-*d*₆ as a deuterated solvent. Melting points were determined in open capillaries using a BUCHI510 melting point apparatus. Thin-layer chromatography (TLC) was performed on silica-gel Poly Gram SIL G/UV 254 plates and progress of reactions was monitored by TLC. Fourier transform infrared (FT-IR) spectra were recorded using KBr disks on a JASCO FT-IR 460 Plus spectrophotometer. Elemental compositions were determined with a Leo 1450 VP scanning electron microscope equipped with an SC7620 energy-dispersive spectrometer (SEM-EDS) presenting a 133-eV resolution at 20 kV. Power X-ray diffraction (XRD) was performed on a Bruker D8-Advance X-ray diffractometer



Scheme 1 Synthesis of 5-(aryl)-5*H*-spiro[diindeno[1,2-*b*:2',1'-*e*]pyridine-11,3'-indoline]-2',10,12-trione derivatives in the presence of γ -Fe₂O₃@SiO₂@4-(sulfoamino)butanoic acid as nanocatalyst

with Cu K α ($\lambda = 0.154$ nm) radiation. The magnetic property of γ -Fe₂O₃@SiO₂ was measured with vibrating sample magnetometry/alternating gradient force magnetometry (VSM/AGFM). Thermal gravimetric analysis (TGA) was done on a thermal analyzer with a heating rate of 10 °C min⁻¹ over a temperature range of 25–800 °C under flowing compressed N₂.

Preparation of γ -aminobutyric acid supported on γ -Fe₂O₃@SiO₂ magnetic nanoparticles

Preparation of γ -Fe₂O₃

The Fe₃O₄ nanoparticles were prepared according to a previously reported procedure [19, 20]. FeCl₂·4H₂O (1.25 g) and FeCl₃·6H₂O (3.33 g) were dissolved in water (80 mL) separately, followed by the two iron salt solutions being mixed under continuous stirring (800 rpm). Then, a NH₄OH solution (%25, 70 mL) was drop added to the stirring mixture at room temperature at 3 h and stirred continuously for 1 h; the black products were collected by an external magnet. Then, Fe₃O₄ magnetic nanoparticles (MNPs) were washed three times with water and ethanol and dried at 60 °C for 12 h. Fe₃O₄ nanoparticles at this stage were heated at 300 °C in a furnace for 3 h to convert Fe₃O₄ to sustainable γ -Fe₂O₃ nanoparticles.

Preparation of γ -Fe₂O₃@SiO₂

γ -Fe₂O₃ nanoparticles (1 g) were dispersed in ethanol (40 mL) and the resulting mixture was stirred for 1 h at 40 °C. Subsequently, tetraethyl orthosilicate (TEOS, 2 mL) was charged to the reaction vessel, and the mixture was continuously stirred for 24 h [20]. The silica-coated nanoparticles were collected by an external magnet, followed by washing three times with ethanol and drying at 70 °C in a vacuum for 12 h; γ -Fe₂O₃@SiO₂ was obtained.

Preparation of γ -aminobutyric acid supported on γ -Fe₂O₃@SiO₂ nanoparticles

γ -Fe₂O₃@SiO₂ (800 mg) was dispersed in water (80 mL) under ultrasonic irradiation for 30 min. Subsequently, γ -aminobutyric acid (1 g) was charged to the reaction vessel and the mixture was continuously stirred for 16 h at 90 °C. γ -Fe₂O₃@SiO₂- γ -aminobutyric acid nanoparticles were removed from the reaction solution using an external magnet and washed several times with water and ethanol and dried at 60 °C.

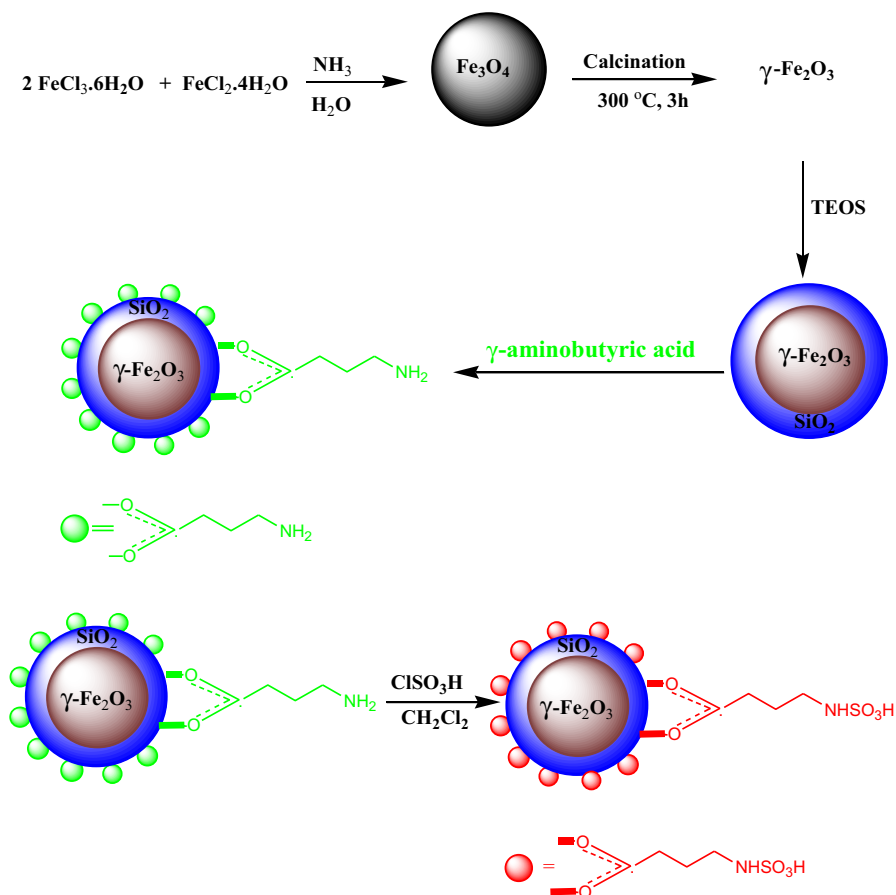
Conversion of the γ -Fe₂O₃@SiO₂- γ -aminobutyric acid MNPs to γ -Fe₂O₃@SiO₂@4-(sulfoamino)butanoic acid MNPs

A dispersion of 800 mg of the prepared magnetic γ -Fe₂O₃@SiO₂- γ -aminobutyric acid nanoparticles in 40 mL chloroform was ultra-sonicated for 30 min. Then, chlorosulfonic acid (0.5 mL, 7.5 mmol) was added drop-wise and the resulting

reaction mixture was stirred for 4 h. The resulted brown powder was separated using an external magnet, washed with ethanol several times, and dried 12 h at 60 °C (Scheme 2). The structure of successful synthesis of $\gamma\text{-Fe}_2\text{O}_3\text{@SiO}_2\text{-}\gamma\text{-aminobutyric acid}$ MNPs was confirmed by FT-IR, EDX, SEM, VSM, XRD, and TGA analysis.

General procedure for the direct synthesis of 5-(aryl)-5*H*-spiro[diindeno[1,2-*b*:2',1'-*e*]pyridine-11,3'-indoline]-2',10,12-trione derivatives using $\gamma\text{-Fe}_2\text{O}_3\text{@SiO}_2\text{-4-(sulfoamino)butanoic acid}$ nanoparticles

$\gamma\text{-Fe}_2\text{O}_3\text{@SiO}_2\text{-4-(sulfoamino)butanoic acid}$ MNPs (5 mg) were added to a mixture 1,3-indandione (1.0 mmol), isatin (0.5 mmol), and aniline (0.5 mmol) in water (3 mL). The reaction mixture was stirred at 60 °C in an oil bath. After completion of the reaction, the reaction mixture was cooled to room temperature. The solid crude product was separated by filtration, and ethanol was added to the



Scheme 2 Synthesis of $\gamma\text{-Fe}_2\text{O}_3\text{@SiO}_2\text{-4-(sulfoamino)butanoic acid}$ as nanocatalyst

reaction mixture and heated to separate $\gamma\text{-Fe}_2\text{O}_3\text{@SiO}_2\text{@4-(sulfoamino)butanoic}$ acid by an external magnet. The nanocatalyst was washed with ethanol three times and dried. The warm ethanolic solution containing crude product was cooled until precipitated pure product was formed. The known pure products were characterized and their physical data were compared with those of known compounds.

Experimental characterization data and spectra of the new compounds

5-(3,4-dichlorophenyl)-5H-spiro[diindeno[1,2-b:2',1'-e]pyridine-11,3'-indoline]-2',10,12-trione (4k) Red powder; mp > 300 °C. IR (KBr; $\nu_{\text{max}}/\text{cm}^{-1}$): 3398, 1710, 1623. ^1H NMR (300 MHz, $\text{DMSO-}d_6$): δ_{H} (ppm) 5.66 (2H, d, $J = 6.9$ Hz, H-Ar), 6.87–8.74 (13H, m, H-Ar), 10.67 (1H, s, NH). ^{13}C NMR (75 MHz, $\text{DMSO-}d_6$): δ_{C} (ppm) 46.07, 97.80, 109.54, 112.26, 121.80, 121.98, 122.13, 125.14, 127.42, 129.12, 130.83, 132.67, 133.31, 134.76, 135.23, 135.35, 136.48, 138.03, 142.58, 156.94, 177.83, 190.06.

5-(3,5-dichlorophenyl)-5H-spiro[diindeno[1,2-b:2',1'-e]pyridine-11,3'-indoline]-2',10,12-trione (4l) Red powder; mp > 300 °C. IR (KBr; $\nu_{\text{max}}/\text{cm}^{-1}$): 3394, 1702, 1690. ^1H NMR (300 MHz, $\text{DMSO-}d_6$): δ_{H} (ppm) 5.75 (2H, d, $J = 6.9$ Hz, H-Ar), 6.87–8.56 (13H, m, H-Ar), 10.67 (1H, s, NH). ^{13}C NMR (75 MHz, $\text{DMSO-}d_6$): δ_{C} (ppm) 46.01, 109.54, 112.26, 121.62, 121.99, 122.21, 125.17, 129.14, 130.06, 130.89, 132.41, 132.64, 133.31, 134.75, 135.88, 136.43, 140.29, 142.53, 155.76, 177.84, 190.04.

5'-chloro-5-(3,5-dichlorophenyl)-5H-spiro[diindeno[1,2-b:2',1'-e]pyridine-11,3'-indoline]-2',10,12-trione (4m) Red powder; mp > 300 °C. IR (KBr; $\nu_{\text{max}}/\text{cm}^{-1}$): 3377, 1725, 1698. ^1H NMR (300 MHz, $\text{DMSO-}d_6$): δ_{H} (ppm) 5.66 (2H, d, $J = 6.9$ Hz, H-Ar), 6.89–8.57 (12H, m, H-Ar), 10.82 (1H, s, NH). ^{13}C NMR (75 MHz, $\text{DMSO-}d_6$): δ_{C} (ppm) 46.25, 110.97, 111.57, 121.76, 122.33, 125.26, 126.25, 129.02, 129.85, 130.06, 131.04, 132.43, 132.58, 133.37, 135.84, 136.36, 140.23, 141.26, 156.12, 177.68, 190.04.

5'-chloro-5-(3-chlorophenyl)-5H-spiro[diindeno[1,2-b:2',1'-e]pyridine-11,3'-indoline]-2',10,12-trione (4n) Red powder; mp > 300 °C. IR (KBr; $\nu_{\text{max}}/\text{cm}^{-1}$): 3360, 1702, 1687. ^1H NMR (300 MHz, $\text{DMSO-}d_6$): δ_{H} (ppm) 5.55 (2H, d, $J = 7.5$ Hz, H-Ar), 6.89–8.97 (12H, m, H-Ar), 10.82 (1H, s, NH). ^{13}C NMR (75 MHz, $\text{DMSO-}d_6$): δ_{C} (ppm) 46.32, 110.93, 111.42, 121.81, 122.24, 124.91, 125.30, 126.57, 127.17, 128.98, 129.38, 131.48, 133.17, 134.14, 136.43, 136.48, 139.49, 141.59, 142.72, 143.47, 156.41, 177.80, 190.06.

Results and discussion

New $\gamma\text{-Fe}_2\text{O}_3\text{@SiO}_2\text{@4-(sulfoamino)butanoic}$ acid as a catalyst was synthesized based on the following procedure (Scheme 2). The magnetic nanocatalyst was characterized using different techniques such as XRD, SEM, EDS, VSM, TGA, and

FT-IR. The XRD patterns of $\gamma\text{-Fe}_2\text{O}_3$, $\gamma\text{-Fe}_2\text{O}_3\text{@SiO}_2$, $\gamma\text{-Fe}_2\text{O}_3\text{@SiO}_2\text{-}\gamma\text{-aminobutyric acid}$, and $\gamma\text{-Fe}_2\text{O}_3\text{@SiO}_2\text{-4-(sulfoamino)butanoic acid}$ had six characteristic peaks which have good accordance with the cubic structure of maghemite ($\gamma\text{-Fe}_2\text{O}_3$; JCPDS file No 04-0755; Fig. 1). The positions of all the peaks indicated retention of the crystalline structure during functionalization of the MNPs and the grafting process did not change the phase of the $\gamma\text{-Fe}_2\text{O}_3$ nanoparticles. The XRD patterns of $\gamma\text{-Fe}_2\text{O}_3\text{@SiO}_2$ and $\gamma\text{-Fe}_2\text{O}_3\text{@SiO}_2\text{-4-(sulfoamino)butanoic acid}$ confirmed that SiO_2 and 4-(sulfoamino)butanoic acid formed an amorphous phase; their patterns showed only a crystalline pattern for the $\gamma\text{-Fe}_2\text{O}_3$ nanoparticles (Fig. 1).

Figure 2 presents the field-emission SEM (FE-SEM) image of $\gamma\text{-Fe}_2\text{O}_3\text{@SiO}_2\text{-4-(sulfoamino)butanoic acid}$ showing a spherical morphology (Fig. 2a) and an average nanoparticles size of 14 nm using a histogram curve (Fig. 2b).

The components of the $\gamma\text{-Fe}_2\text{O}_3\text{@SiO}_2\text{-4-(sulfoamino)butanoic acid}$ were analyzed using EDS. EDS basically gives quality elemental information [21]. The EDS spectrum in Fig. 3 shows the presence of Fe, O, Si, C, S, and N atoms in the catalyst.

The VSM diagram shows the magnetic properties of the synthesis catalyst (Fig. 4). The hysteresis loops of $\gamma\text{-Fe}_2\text{O}_3\text{@SiO}_2\text{-4-(sulfoamino)butanoic acid}$ were measured. Magnetization (emu g^{-1}) as a function of applied field (Oe) is depicted in Fig. 4 with the confined field from $-10,000$ to $10,000$ Oe. The superparamagnetic behavior of $\gamma\text{-Fe}_2\text{O}_3\text{@SiO}_2\text{-4-(sulfoamino)butanoic acid}$ nanocrystals illustrates a small particle size. As can be observed, the saturation magnetization value of $\gamma\text{-Fe}_2\text{O}_3\text{@SiO}_2\text{-4-(sulfoamino)butanoic acid}$ is 13 amu g^{-1} .

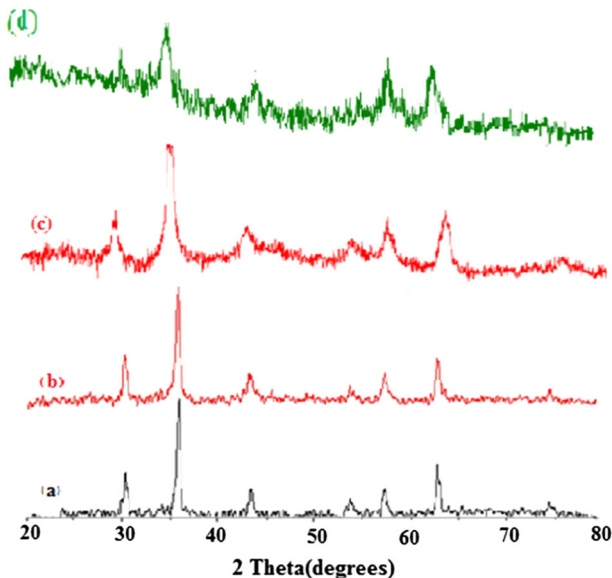
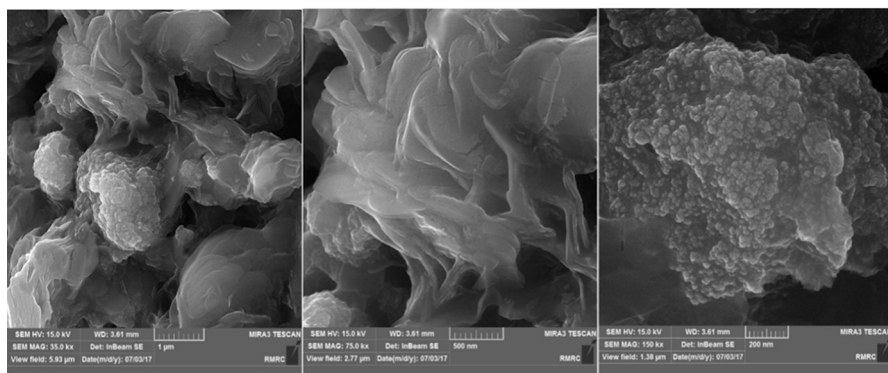


Fig. 1 XRD pattern of **a** $\gamma\text{-Fe}_2\text{O}_3$, **b** $\gamma\text{-Fe}_2\text{O}_3\text{@SiO}_2$, **c** $\gamma\text{-Fe}_2\text{O}_3\text{@SiO}_2\text{-}\gamma\text{-aminobutyric acid}$, and **d** $\gamma\text{-Fe}_2\text{O}_3\text{@SiO}_2\text{-4-(sulfoamino)butanoic acid}$

(a)



(b)

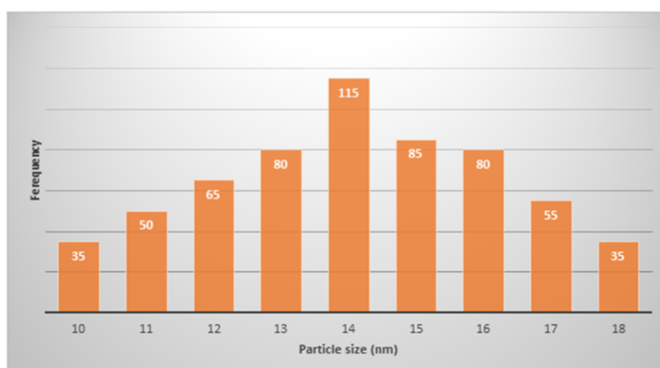


Fig. 2 **a** FE-SEM image of $\gamma\text{-Fe}_2\text{O}_3@4\text{-(sulfoamino)butanoic acid}$; **b** Particle size distribution histogram of $\gamma\text{-Fe}_2\text{O}_3@4\text{-(sulfoamino)butanoic acid}$

The thermal stability of the $\gamma\text{-Fe}_2\text{O}_3@4\text{-(sulfoamino)butanoic acid}$ was investigated by TGA (Fig. 5). Small weight loss occurs below 180 °C and is due to physically adsorbed water. There are two exothermic peaks accompanied with a mass loss of 42% in the temperature range of 180–620 °C in the differential thermal analysis (DTA) curve of $\gamma\text{-Fe}_2\text{O}_3@4\text{-(sulfoamino)butanoic acid}$. These peaks were mainly attributed to the decomposition of organic groups grafted to the $\gamma\text{-Fe}_2\text{O}_3@4\text{-(sulfoamino)butanoic acid}$ surface and $\text{-SO}_3\text{H}$ loaded on aminopropyl groups. The peak higher than 620 °C most probably corresponds to a phase transition in which the amorphous phase is converted to a crystalline phase.

The characterization of $\gamma\text{-Fe}_2\text{O}_3@4\text{-(sulfoamino)butanoic acid}$ was confirmed by FT-IR spectroscopy (Fig. 6) which showed spectra of: (a) $\gamma\text{-Fe}_2\text{O}_3@4\text{-(sulfoamino)butanoic acid}$, (b) $\gamma\text{-Fe}_2\text{O}_3@4\text{-(sulfoamino)butanoic acid}$, and (c) $\gamma\text{-aminobutyric acid}$. The C–H stretching vibration peak appears at 2930 cm^{-1} . The Fe–O stretching vibration was observed $550\text{--}650\text{ cm}^{-1}$ and the stretching mode of Si–O–Si showed a strong broad peak at about $1099\text{--}1220\text{ cm}^{-1}$. The functionalization of SO_3H groups on the MNPs- $\gamma\text{-aminobutyric acid}$ surface was confirmed by the absorption of S–O and S=O stretching bands of the $\text{-SO}_3\text{H}$ moiety at $998\text{--}1220\text{ cm}^{-1}$ in the FT-IR

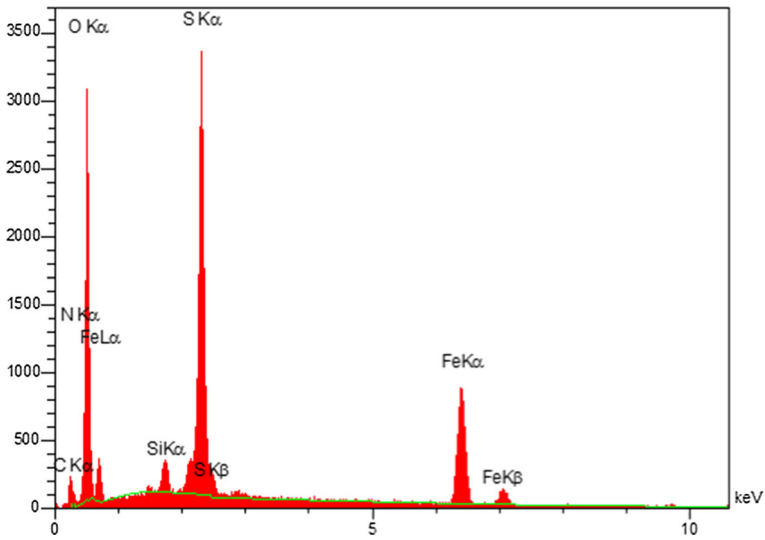


Fig. 3 EDS spectrum of γ -Fe₂O₃@SiO₂@4-(sulfoamino)butanoic acid

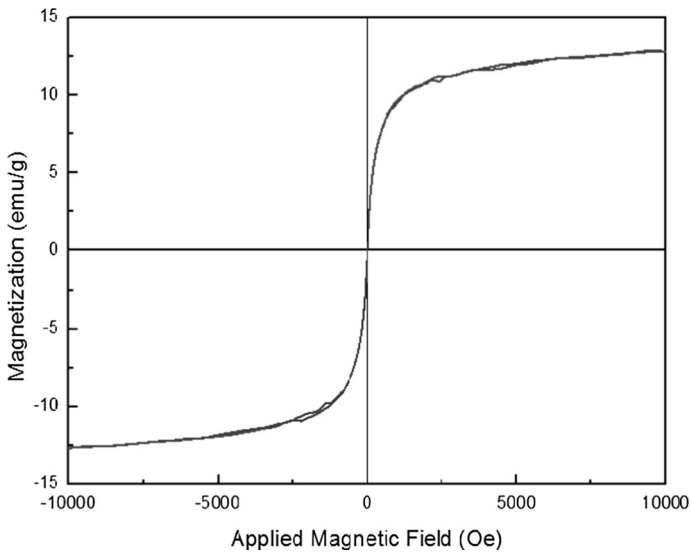


Fig. 4 VSM diagram of γ -Fe₂O₃@SiO₂@4-(sulfoamino)butanoic acid

spectrum. In addition, in the spectrum of γ -Fe₂O₃@SiO₂@4-(sulfoamino)butanoic acid, the peak at 3405 cm⁻¹ was probably attributed to the -SO₂-OH groups, which is overlapped by the C-H stretching vibration.

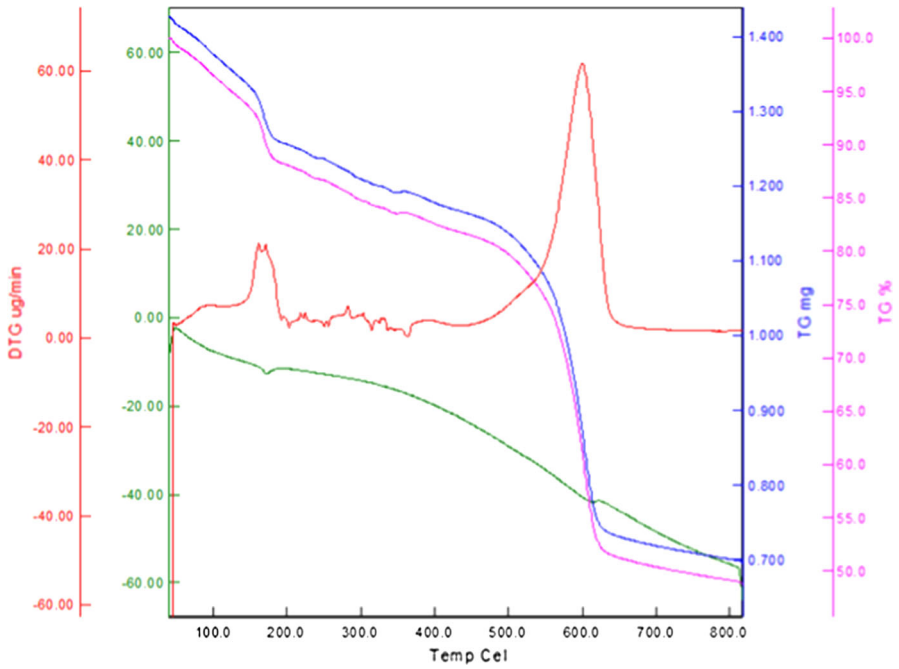


Fig. 5 Thermogravimetric of $\gamma\text{-Fe}_2\text{O}_3\text{@SiO}_2\text{@4-(sulfoamino)butanoic acid}$

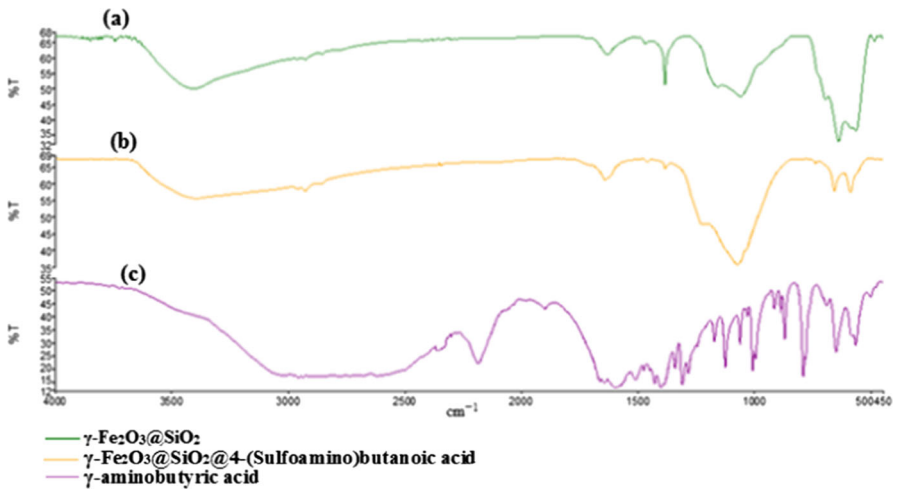
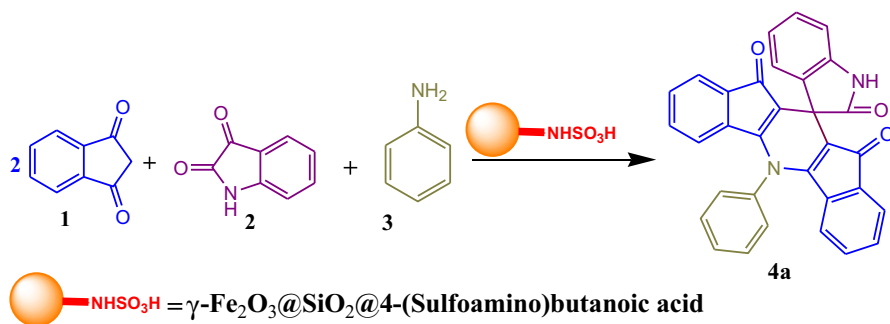


Fig. 6 FT-IR spectra: **a** $\gamma\text{-Fe}_2\text{O}_3\text{@SiO}_2$, **b** $\gamma\text{-Fe}_2\text{O}_3\text{@SiO}_2\text{@4-(sulfoamino)butanoic acid}$, and **c** $\gamma\text{-aminobutyric acid}$



Scheme 3 Synthesis of 5-phenyl-5H-spiro[diindenol[1,2-*b*:2',1'-*e*]pyridine-11,3'-indoline]-2',10,12-trione

Optimization of the reaction conditions

To evaluate the activity of the $\gamma\text{-Fe}_2\text{O}_3\text{@SiO}_2\text{@4-(sulfoamino)butanoic acid}$ as nanocatalyst, firstly, the one-pot and *pseudo* four-component reaction of 1,3-indandione (1 mmol), isatin (0.5 mmol), and aniline (0.5 mmol; Scheme 3) was chosen as a model reaction to optimize the reaction conditions such as molar ratio of the catalyst, temperature, and solvents (Tables 1, 2, and 3).

In order to show the unique catalytic behavior of $\gamma\text{-Fe}_2\text{O}_3\text{@SiO}_2\text{@4-(sulfoamino)butanoic acid}$ as nanocatalyst and to compare its activity with other catalysts, the model reaction was carried out in the presence of catalytic amounts of Fe_3O_4 NMPs, *p*-TSA, AcOH, citric acid, sulfamic acid, PEG-OSO₃H, γ -aminobutyric acid, oxalic acid dihydrate:proline, and $\text{FeCl}_3\cdot 6\text{H}_2\text{O}$ in different solvents and also solvent-free conditions. The results are summarized in Table 1. With regard to Table 1, the $\gamma\text{-Fe}_2\text{O}_3\text{@SiO}_2\text{@4-(sulfoamino)butanoic acid}$ showed better activity and excellent yield of the product (95%) in a minimum time period (20 min) was obtained at 60 °C in aqueous media in the presence of 5 mg of $\gamma\text{-Fe}_2\text{O}_3\text{@SiO}_2\text{@4-(sulfoamino)butanoic acid}$ (Table 1, entry 6). The reaction in the presence of γ -aminobutyric acid as a non-supported catalyst on MNPs gave the desired product in moderate yield (50%) at 80 °C. Thus, immobilization of γ -aminobutyric acid on $\gamma\text{-Fe}_2\text{O}_3\text{@SiO}_2$ increased the activity of the organocatalyst and enabled recyclability of the catalyst (Table 1, entry 11). We also examined the model reaction in the absence of any catalyst (Table 1, entry 12), the experimental result of which showed that the catalyst is necessary for preparation of the desired product.

In terms of choosing the best solvent for the reaction of 1,3-indandione (1 mmol), isatin (0.5 mmol), and aniline (0.5 mmol; Scheme 3), different solvents were studied in the presence of $\gamma\text{-Fe}_2\text{O}_3\text{@SiO}_2\text{@4-(sulfoamino)butanoic acid}$ (Table 2). The best result was obtained after 20 min in aqueous media at 60 °C with excellent yield of the product (95%) in water (Table 2, entry 5). Water is a more appropriate green solvent for synthesis of the desired product because of cost, safety, and environmental concerns.

Varying the amount of $\gamma\text{-Fe}_2\text{O}_3\text{@SiO}_2\text{@4-(sulfoamino)butanoic acid}$ as nano-magnetic catalyst was investigated for the synthesis of 5-(aryl)-5H-

Table 1 Preparation of 5-phenyl-5*H*-spiro[diindeno[1,2-*b*:2',1'-*e*]pyridine-11,3'-indoline]-2',10,12-trione in the presence of γ -Fe₂O₃@SiO₂@4-(sulfoamino)butanoic acid, Fe₃O₄ MNPs, *p*-TSA, AcOH, citric acid, sulfamic acid, PEG-OSO₃H, γ -aminobutyric acid, oxalic acid dihydrate:proline, and FeCl₃·6H₂O in different solvents and solvent-free conditions

Entry	Catalyst	Conditions	Time	Yield (%) ^{a,b}	Citation
1	FeCl ₃ ·6H ₂ O (7 mol%)	CH ₃ CN (reflux)	2 h	60	–
2	Fe ₃ O ₄ MNPs (5 mol%)	Water (80 °C)	2 h	75	[24]
3	<i>p</i> -TSA (30 mol%)	CH ₃ CN (reflux)	1 h	81	–
4	AcOH (30 mol%)	Water (reflux)	1 h	60	[23]
5	PEG-OSO ₃ H (20 mol%)	Water (80 °C)	10 min	90	[23]
6	γ -Fe ₂ O ₃ @SiO ₂ @4-(sulfoamino)butanoic acid (5 mg)	Water (60 °C)	20 min	95	–
7	Oxalic acid dihydrate: proline(5 mL)	Water (80 °C)	20 min	94	[22]
8	γ -Fe ₂ O ₃ @SiO ₂ @4-(sulfoamino)butanoic acid(5 mg)	Solvent-free (90 °C)	30 min	85	–
9	Sulfamic acid (25 mol%)	Water (80 °C)	1 h	65	–
10	Citric acid (20 mol%)	Water (80 °C)	1 h	50	–
11	γ -Aminobutyric acid (25 mol%)	Water (80 °C)	1 h	50	–
12	No catalyst	Water (100 °C)	24 h	Trace	–

^aReaction conditions: 1,3-indandione (1 mmol), isatin (0.5 mmol), and aniline (0.5 mmol) in different conditions

^bYield refers to isolated pure products

Table 2 Preparation of 5-(aryl)-5*H*-spiro[diindeno[1,2-*b*:2',1'-*e*]pyridine-11,3'-indoline]-2',10,12-trione in the presence of γ -Fe₂O₃@SiO₂@4-(sulfoamino)butanoic acid (5 mg) in different solvents and also solvent-free conditions

Entry	Solvent	Time (min)	Temperature (°C)	Yield (%) ^{a,b}
1	EtOH (3 mL)	60	70	75
2	CH ₃ CN (3 mL)	60	70	80
3	CH ₂ Cl ₂ (3 mL)	120	Reflux	25
4	Solvent-free	30	90	85
5	H ₂ O (3 mL)	20	60	95
6	H ₂ O:EtOH (1:1; 3 mL)	45	70	80

^aReaction conditions: 1,3-indandione (1 mmol), isatin (0.5 mmol), and aniline (0.5 mmol)

^bYield refers to isolated pure products

spiro[diindeno[1,2-*b*:2',1'-*e*]pyridine-11,3'-indoline]-2',10,12-trione in water media (Table 3). The optimum amount of the catalyst for maximum conversion was found to be 5 mg at 60 °C (Table 3, entry 4). Increasing the amount of γ -Fe₂O₃@SiO₂@4-(sulfoamino)butanoic acid had no effect in the product yield (Table 3, entry 5). For optimization of the temperature, the reaction was performed at different

Table 3 Optimization the amount of the catalyst and also selecting the best temperature for the preparation of 5-(aryl)-5*H*-spiro[diindeno[1,2-*b*:2',1'-*e*]pyridine-11,3'-indoline]-2',10,12-trione in aqueous media

Entry	Catalyst (mg)	Temperature (°C)	Time (min)	Yield (%) ^{a,b}
1	2	60	50	75
2	3	60	45	82
3	4	60	30	87
4	5	60	20	95
5	7	60	15	95
6	5	50	35	75
7	5	70	15	95

^aReaction condition: 1,3-indandione (1 mmol), isatin (0.5 mmol), and aniline (0.5 mmol) in water (3 mL) as solvent

^bYield refers to isolated pure products

temperatures (50, 60, and 70 °C; Table 3) using γ -Fe₂O₃@SiO₂@4-(sulfoamino)butanoic acid (5 mg) in water (3 mL); the best result was obtained at 60 °C (Table 3, entry 4).

Secondly, after optimizing the reaction conditions, the generality of this procedure was studied on a wide range of aromatic amines and isatins for preparation of 5-(aryl)-5*H*-spiro[diindeno[1,2-*b*:2',1'-*e*]pyridine-11,3'-indoline]-2',10,12-trione derivatives (Table 4). It was observed that the desired products were obtained in high to excellent yields with short reaction times (Table 4, entries 1–14).

The mechanism for the formation of the desired product was suggested according to the literature [24]. First, condensation between 1,3-indandione (1) and isatin (2) formed intermediate (I). Second, the condensation reaction of (I) with another molecule of 1,3-indandione produced compound (II). In the following, enamine (III) was formed from condensation of amine with a carbonyl group (II). Then, the intramolecular cyclization of (III) led to formation of the final desired products (Scheme 4).

The recyclability of γ -Fe₂O₃@SiO₂@4-(sulfoamino)butanoic acid as nanocatalyst was examined in the one-pot *pseudo* four-component synthesis of 5-(phenyl)-5*H*-spiro[diindeno[1,2-*b*:2',1'-*e*]pyridine-11,3'-indoline]-2',10,12-trione under optimized conditions (model reaction). After completion of the reaction, the reaction mixture was cooled to room temperature. The solid crude product was separated by filtration, and ethanol was added to the reaction mixture and heated to separate γ -Fe₂O₃@SiO₂@4-(sulfoamino)butanoic acid by external magnet. The nanocatalyst was washed with ethanol for three times and dried. The recoverable nanocatalyst was used for other reaction runs. As shown in Fig. 7, the reusable nanocatalyst was

Table 4 Synthesis of 5-(aryl)-5*H*-spiro[diindeno[1,2-*b*:2',1'-*e*]pyridine-11,3'-indoline]-2',10,12-trione derivatives in the presence of γ -Fe₂O₃@SiO₂@4-(sulfoamino)butanoic acid (5 mg) as nanomagnetic catalyst at 60 °C in water (3 mL) as a green solvent

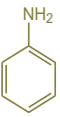
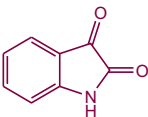
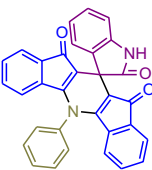
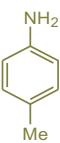
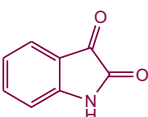
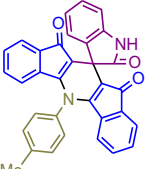
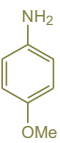
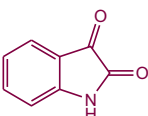
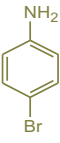
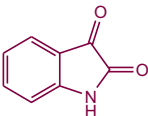
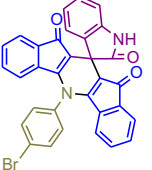
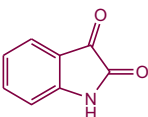
Entry	amine	isatin	product	Time (min)	Yield (%) ^{a,b}	Observed M.p (°C)	Lit. M.p (°C), [Ref]
1			 4a	20	95	>300	>300 [24]
2			 4b	20	98	>300	>300 [24]
3			 4c	15	98	>300	>300 [24]
4			 4d	20	94	>300	>300 [24]
5			 4e	25	93	>300	>300 [24]

Table 4 continued

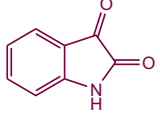
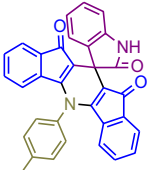
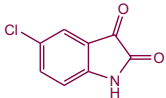
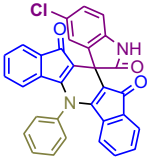
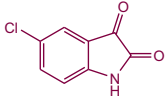
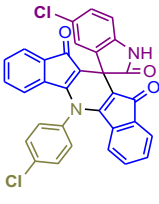
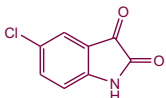
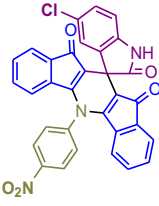
6			 4f	20	95	>300	>300 [22]
7			 4g	20	94	>300	>300 [22]
8			 4h	20	94	>300	>300 [22]
9			 4i	25	93	>300	>300 [22]

Table 4 continued

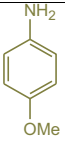
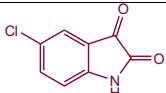
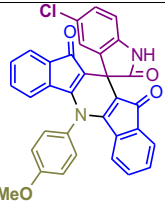
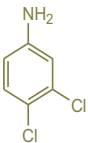
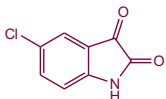
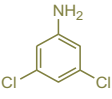
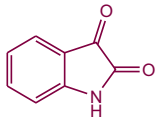
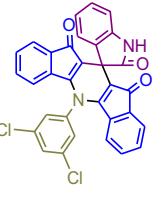
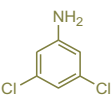
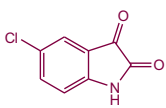
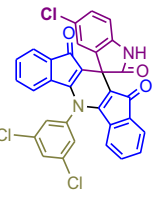
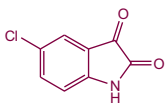
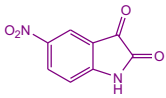
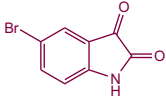
10			 4j	18	98	>300	>300 [22]
11			 4k	25	94	>300	New Compound
12			 4l	20	95	>300	New Compound
13			 4m	25	93	>300	New Compound
14			 4n	20	94	>300	New Compound

Table 4 continued

15			 4o	19	93	>300	>300 [23]
16			 4p	18	92	>300	>300 [23]

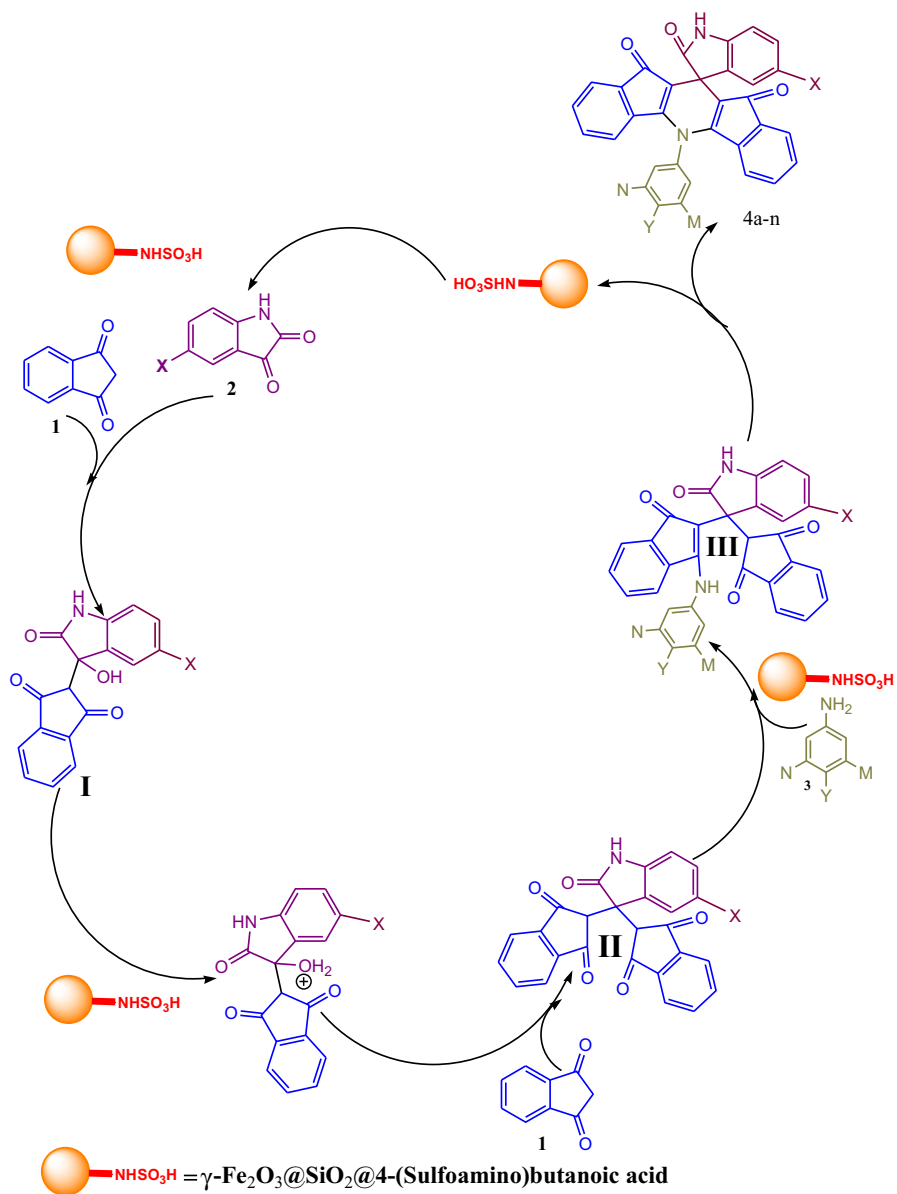
^aReaction conditions: 1,3-indandione (1 mmol), isatins (0.5 mmol) and aromatic amines (0.5 mmol) in water (3 mL)

^bYield refer to isolated pure products

used for at least five runs. The catalyst kept its stability without any loss of any significant activity.

Conclusion

$\gamma\text{-Fe}_2\text{O}_3\text{@SiO}_2\text{-}4\text{-(sulfoamino)butanoic acid}$ as a novel organometallic heterogeneous nanomagnetic catalyst has been successfully synthesized and characterized by several techniques such as XRD, FT-IR, VSM, FE-SEM, EDS, and TGA. This efficient nano-organometallic catalyst was successfully used for the *pseudo four*-component preparation of 5-(aryl)-5*H*-spiro[diindeno[1,2-*b*:2',1'-*e*]pyridine-11,3'-indoline]-2',10,12-trione derivatives under green conditions in aqueous media. Easy reaction conditions, simple work-up, or purification, excellent yields, high purity of the desired product, and short reaction times are some advantages of this protocol. The superparamagnetic nanocatalyst is magnetically separable and stable in the reaction media without detectable activity loss.



Scheme 4 The proposed mechanism for the synthesis of 5-(aryl)-5*H*-spiro[diindeno[1,2-*b*:2',1'-*e*]pyridine-11,3'-indoline]-2',10,12-trione in the presence of $\gamma\text{-Fe}_2\text{O}_3@\text{SiO}_2@4\text{-(sulfoamino)butanoic acid}$ as nanocatalyst

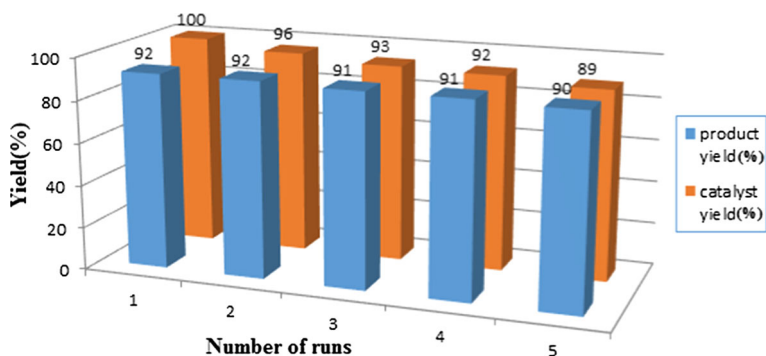


Fig. 7 Reusability of γ -Fe₂O₃@SiO₂@4-(sulfoamino)butanoic acid as nanomagnetic catalyst

Acknowledgements We are grateful for the financial support from the Research Council of University of Sistan and Baluchestan.

References

1. L. Wu, A. Mendoza-Garcia, Q. Li, S. Sun, *Chem. Rev.* **116**, 10473 (2016)
2. A.S. Paulus, R. Heinzler, H.W. Ooi, M. Franzreb, *ACS Appl. Mater. Interfaces* **7**, 14279 (2015)
3. A.P. Tiwari, S.J. Ghosh, S.H. Pawar, *Anal. Methods* **7**, 10109 (2015)
4. Q. Luo, X. Xiao, X. Dai, Z. Duan, D. Pan, H. Zhu, X. Li, L. Sun, K. Luo, Q. Gong, *ACS Appl. Mater. Interfaces* **10**, 1575 (2018)
5. S.V. Sokolov, E. Kätelhön, R.G. Compton, *J. Phys. Chem. C* **119**, 25093 (2015)
6. M.F. Silva, A.A.W. Hechenleitner, J.M. Irache, A.J.A. de Oliveira, E.A. Gómez Pineda, *Mater. Res.* **18**, 1400 (2015)
7. X. Yao, J. Jing, F. Liang, Z. Yang, *Macromolecules* **49**, 9618 (2016)
8. A. Taghvimi, H. Hamishehkar, *J. Chromatogr. B* **1041–1042**, 113 (2017)
9. S. Laurent, D. Forge, M. Port, A. Roch, C. Robic, L.V. Elst, R.N. Muller, *Chem. Rev.* **108**, 2064 (2008)
10. R.K. Sharma, M. Yadav, M.B. Gawande, in *ACS Symp. Ser.* 2016, p. 1
11. N. Pal, A. Bhaumik, *RSC Adv.* **5**, 24363 (2015)
12. N. Taheri, F. Heidarizadeh, A. Kiasat, *J. Magn. Mater.* **428**, 481 (2017)
13. M. Abdollahi-Alibeik, A. Rezaeipoor-Anari, *J. Magn. Mater.* **398**, 205 (2016)
14. W. Wu, C.Z. Jiang, V.A.L. Roy, *Nanoscale* **8**, 9421 (2016)
15. P. Saravanan, K. Jayamoorthy, S. Anandakumar, *J. Lumin.* **178**, 241 (2016)
16. D.G. Wang, C. Deraedt, J. Ruiz, D. Astruc, *Acc. Chem. Res.* **48**, 1871 (2016)
17. M. Zhang, Y.H. Liu, Z.R. Shang, H.C. Hu, Z.H. Zhang, *Catal. Commun.* **88**, 39 (2017)
18. M. Zhang, P. Liu, Y.H. Liu, Z.R. Shang, H.C. Hu, Z.H. Zhang, *RSC Adv.* **6**, 106160 (2016)
19. K.M. Ho, P. Li, *Langmuir* **24**, 1801 (2008)
20. K. Azizi, A. Heydari, *RSC Adv.* **4**, 8812 (2008)
21. K. Tsuchi, J. Injuk, R.V. Grieken, *X-Ray Spectrometry: Recent Technological Advances* (Wiley, Hoboken, 2005)
22. D.R. Chandam, A.G. Mulik, D.R. Patil, A.P. Patravale, D.R. Kumbhar, M.B. Deshmukh, *J. Mol. Liq.* **219**, 573 (2016)
23. J. Sindhu, H. Singh, M. Khurana, *Synth. Commun.* **45**, 202 (2015)
24. R. Ghahremanzadeh, G. Imani Shakibaei, S. Ahadi, A. Bazgir, *J. Comb. Chem.* **12**, 191 (2010)

Affiliations

Hadi Mohammadi¹ · Hamid Reza Shaterian¹ 

✉ Hamid Reza Shaterian
hrshaterian@chem.usb.ac.ir

¹ Department of Chemistry, Faculty of Sciences, University of Sistan and Baluchestan,
P.O. Box 98135-674, Zahedan, Iran